Ioffe Institute
6th Int. Symp. "Nanostructures: Physics and Technology"
St Petersburg, Russia, June 22–26, 1998.

Quantum-dot cellular automata — experimental demonstration of a functional cell

A. O. Orlov, I. Amlani, G. L. Snider, G. H. Bernstein, C. S. Lent, J. L. Merz, and W. Porod

Department of Electrical Engineering, University of Notre Dame, Notre Dame, IN 46556 USA

Abstract. The experimental demonstration of a basic cell of Quantum-Dot Cellular Automata, a transistorless computation paradigm is presented. The device studied is a six-dot quantum-dot cellular system consisting of a four-dot QCA cell and two electrometer dots. The system is fabricated using metal dots, connected by capacitors and tunnel junctions. The operation of a basic cell is confirmed by the externally detected change of the cell polarization controlled by the input signal. The cell exhibits a bistable response, with more than 80% charge polarization within a cell.

In the last 30 years the microelectronics industry has made dramatic improvements in the speed and size of electronic devices, and the achievement of ever higher levels of integration requires a further increase in the number of devices fabricated on a chip. Since the early 1970s the device of choice for high levels of integration has been the field effect transistor (FET), and while the FET of today is a vast improvement over that of 1970, it is still a current switch like the mechanical relays first used to encode binary information. At gate lengths below 0.1 μm, FETs will begin to encounter fundamental effects which lead to performance degradation. One alternative approach which could allow the microelectronics industry to maintain continued growth in device density would be a the change from the FET-based paradigm to one based on nanostructures. Here, instead of fighting the effects that come with feature size reduction, these effects are used to advantage. One nanostructure paradigm, proposed by Lent et al. [1, 2], is Quantum-Dot Cellular Automata (QCA), which employs arrays of coupled quantum dots for binary computations [3, 4]. The advantage of QCA lies in the extremely high packing densities possible due to the small size of the dots, the simplified interconnection, and the extremely low power-delay product which can be arbitrarily reduced by adiabatic switching [5]. Using QCA cells with dots of 20 nm diameter, an entire full adder can be placed within 1 μm^2, approximately the area of a single 0.07 μm gate length FET.

A basic QCA cell consists of four quantum dots located at the corners of a square, coupled by tunnel barriers. If the cell is charged with two excess electrons among the four dots, Coulomb repulsion will force the electrons to opposite corners. There are thus two energetically equivalent "polarizations", as shown in Fig. 1a, which can be labeled logic "0" and "1". By properly arranging cells so that the polarization of one cell sets the polarization of a nearby cell, it is possible to implement all combinational logic functions. Since the cells communicate only with their nearest neighbors, there is no need for long interconnect lines. The inputs are applied to the cells at the edge of the system and the computation proceeds until the output appears at cells at the edge of the QCA array.

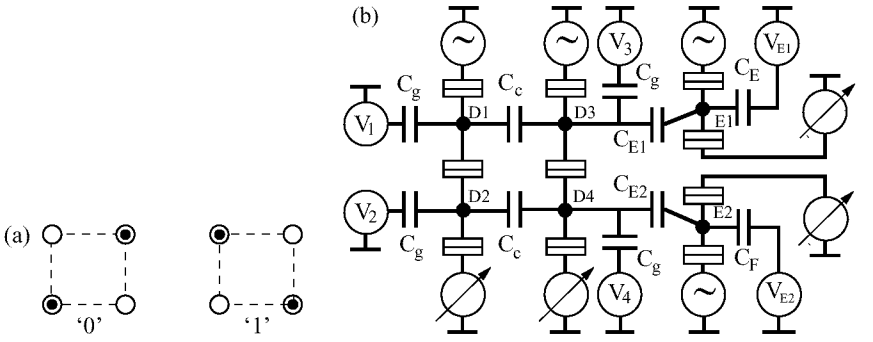

Fig 1. (a) Basic four-dot QCA cell showing the two possible polarizations. (b) Schematic diagram of the four-dot QCA cell with two electrometers.

We study a QCA cell fabricated using aluminum islands with aluminum-oxide tunnel junctions, grown on an oxidized silicon wafer. The fabrication used standard electron beam lithography and shadow evaporation to form the islands and tunnel junctions [6], with typical junction area of $50 \times 50\,\mathrm{nm}^2$. The first step in the development of QCA systems was recently demonstrated in [7] where we showed the possibility to switch the localization of an electron in a double-dot (DD) by swapping an electron in the input dots capacitively coupled to DD [7]. A schematic diagram of the improved device — the four-dot QCA cell with additional electrometers is shown in Fig. 1b. The four dots of the QCA cell consist of two DDs, where the dots are joined by a tunnel junction. This breaks the QCA cell into two half-cells, where electrons are allowed to tunnel "vertically" between dots, but not "horizontally". The input voltages V_1 and V_2 are connected to D_1D_2, which form the input half-cell. D_1D_2 is connected capacitively to the output half-cell D_3D_4, which is in turn capacitively coupled to the electrometers E_1 and E_2. Measurements were performed in a dilution refrigerator with a base temperature of 10 mK. Conductances of DDs and electrometers were measured simultaneously using a standard ac lock-in technique with 5 μV excitation, and a magnetic field of 1 T applied to suppress the superconductivity of Al. Capacitances of the circuit were determined from periods of Coulomb-blockade oscillations and IV-measurements [8].

The operation of a QCA cell is best understood by examining the conductance through the input half-cell as a function of the two gate voltages V_1 and V_2, as shown in the contour plot of Fig. 2. A peak in the conductance is observed each time the Coulomb blockade is lifted for the DD system, and due to the capacitive coupling between the dots each peak splits into a double peak. These peaks form the vertices of a hexagonal structure which we refer to as the "honeycomb", delineated by the dotted lines in Fig. 2 [9]. Within each hexagon the electron population of the dots is stable and changes when a border between cells is crossed. The excess electron population can thus be labeled, with the (0,0) hexagon centered at $V_1 = V_2 = 0$ V. A point in the honeycomb defined by a single setting of V_1 and V_2 is called the working point, which defines a particular configuration of electrons. Most important for QCA operation is motion of the working point in the direction shown by the direction V_{diag} in Fig. 2. This movement between the (1,0) and (0,1) hexagon represents the switching of an electron between the top and bottom dot. If working points for each half-cell are on the border between these

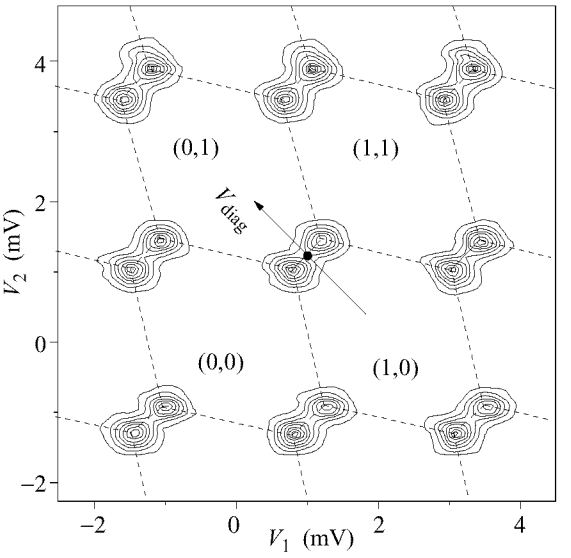

Fig 2. Contour plot of the measured conductance through the input half-cell as a function of V_1 and V_2. The excess electron population is noted as (n_1, n_2).

states, the cell is non-polarized. If we than polarize input DD by applying the control signal to the input gates, the output DD will in turn be polarized to minimize the total energy of the system. The goal of our experiment is to demonstrate QCA operation by using electrodes to force this transition in the input half-cell and then have the potential changes on the input half-cell force an opposite transition in the output half-cell.

To demonstrate QCA operation, it is necessary therefore first to set both DDs in non-polarized state without the input signal. An input signal polarizes the input DD, which in turns polarizes the output DD. The external detectors then measure the position of an excess electron in the output DD.

To accomplish the first part of the task conductance of the DDs is measured as a function of corresponding gate biases, and the appropriate working points are thus chosen. To externally detect the charge state of each dot of D_3D_4 we use additional dots as electrometers [10], capacitively coupled to the output half-cell, as shown in the schematic of Fig. 2. The electrometer operates by detecting small potential changes in the dot being measured. Knowing the capacitance coupling the electrometer to the dot and the electrometer charge sensitivity, it is possible to calculate the potential on the measured dot.

QCA operation is demonstrated by applying a differential voltage to the input half-cell, a positive bias to V_2 and a negative bias to V_1. As this differential voltage is swept along V_{diag}, electrons tunneling one-by-one through D_1D_2 spend more time on D_2, and the electrostatic potential on D_1 and D_2 changes in response to the applied gate voltages and the position of electrons. The potential on D_2 increases with the positive voltage V_2, until an abrupt reset which occurs when an electron enters the dot. Likewise, the potential on dot D_1 also changes as a function of V_1, but with the opposite phase. Since the potentials on D_1 and D_2 act as additional gate voltages for D_3 and D_4, the

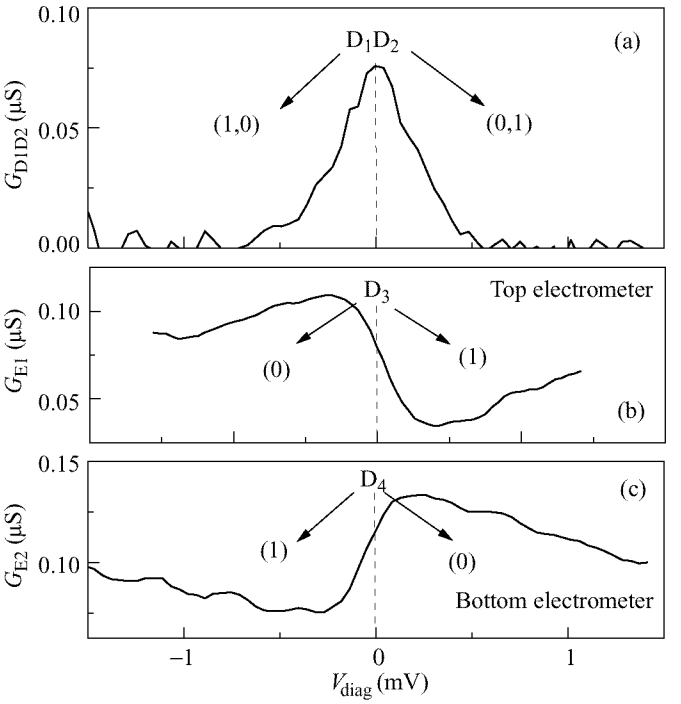

Fig 3. (a) Conductance through the input half-cell versus V_{diag}. The peak indicates the switch of an electron from D_1 to D_2. (b) Conductance through the electrometer E_1 indicating the addition of an electron to D_3. (c) Conductance through electrometer E_2 indicating the removal of an electron from D_4.

honeycomb of the output half-cell will shift in response to potential changes in the input half-cell. For QCA operation a shift must be sufficient to move the D_3D_4 honeycomb so that the working point of the D_3D_4 appears in (0,1) or (1,0) hexagons, depending on polarization of D_1D_2. This represents a switch of an electron in the output half-cell. The switching in the output half-cell will be detected by the two electrometers, where the current in one electrometer will increase as an electron leaves its adjacent dot, while the current in the other electrometer will decrease as an electron enters its adjacent dot. The experimental measurements confirm this behavior, as shown in Fig. 3, which plots the conductance through the input half-cell, along with the conductance through each electrometer as a function of the input voltage V_{diag} ($V_2 = -V_1$). The peak in the conductance through the input half-cell, seen in Fig. 3a as V_2 increases, indicates that an electron has moved from D_1 to D_2. As the electron switches in the input half-cell the conductance of the top electrometer decreases (Fig. 3b), and rises for the bottom electrometer (Fig. 3c). This indicates that an electron has moved from D_4 to D_3 as expected due to the electron switch in the input half-cell. This confirms the polarization change required for QCA operation.

Using the electrometer signal of Fig. 3b we calculate the potential on D_3 as a function of the input differential voltage and compare it with theory. This is plotted in

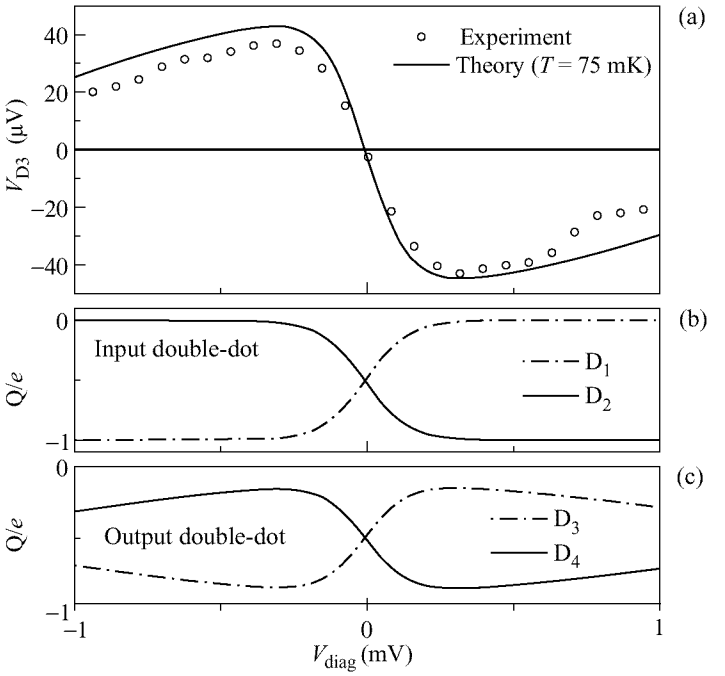

Fig 4. (a) Measured potential on dot D_3 as a function of V_{diag}, along with theory at 75 mK. Calculated excess electron population for (b), the input half-cell D_1 and D_2, and (c), the output half-cell D_3 and D_4, as a function of V_{diag}.

Fig. 4a, along with the theoretically calculated potential at a temperature of 75 mK. At a temperature of 0 K the potential changes are abrupt, while the observed potential shows the effects of thermal smearing, and theory at 75 mK shows good agreement with experiment. The heating of the electron system above the base temperature of the dilution refrigerator is likely due to the applied excitation voltage and noise voltages coupled into the sample by the leads. This effect is commonly seen in measurements of this type [11]. Figures 4b and 4c plot the theoretical excess charge on each of the dots in the input and output half-cells, at 75 mK.

This shows a 80% polarization switch of the QCA cell, and the polarization change can be further improved with an increase in the capacitances coupling input and output half-cells.

A device paradigm based on QCA cells offers the opportunity to break away from FET based logic, and to exploit the quantum effects that come with small size. In QCA approach, logic levels are no longer encoded as voltages but as the position of electrons within a quantum dot cell. QCA cells are scalable to molecular dimensions, and the performance improves as the size shrinks. A QCA cell with molecular dimensions should operate at room temperature since the energy spacings of the dot states will be larger than kT, even at 300 K.

Using metal island dots with oxide tunnel junctions, we have demonstrated the operation of a QCA cell. The cell exhibits a bistable distribution of electrons, and the

polarization of the cell can be switched by externally applied bias voltages.

This work was supported in part by the Defense Advanced Projects Agency, Office of Naval Research (contract No. N00014-95-1-1166), and the National Science Foundation.

References

[1] C. S. Lent et al., *Nanotechnology* **4** 49 (1993).
[2] C. S. Lent and P. D. Tougaw, *Proceedings of the IEEE* **85** 541 (1997).
[3] C. S. Lent and P. D. Tougaw, *J. Appl. Phys.* **74** 6227 (1993).
[4] P. D. Tougaw and C. S. Lent, *J. Appl. Phys.* **75** 1818 (1994).
[5] P. D. Tougaw and C. S. Lent, *J. Appl. Phys.* **80** 4722 (1996).
[6] T. A. Fulton and G. H. Dolan, *Phys. Rev. Lett.* **59** 109 (1987).
[7] A. O. Orlov et al., *Science* **277** 928 (1997).
[8] K. K. Likharev, *IBM J. Res. Dev.* 114 (1988).
[9] H. Pothier et al, *Physica B* **169** 573 (1991).
[10] I. Amlani et al., *Appl. Phys. Lett.* **71** 1730 (1997).
[11] P. Lafarge et al., *Z. Phys. B* **85** 327 (1991).